THE ASTROPHYSICAL JOURNAL, 520:574–591, 1999 August 1
© 1999. The American Astronomical Society. All rights reserved. Printed in U.S.A.

MODELING ELLIPTICAL GALAXIES: PHASE-SPACE CONSTRAINTS ON TWO-COMPONENT (γ_1, γ_2) MODELS

L. CIOTTI[1,2]

Received 1998 October 20; accepted 1999 March 11

ABSTRACT

In the context of the study of the properties of the mutual mass distribution of the bright and dark matter in elliptical galaxies, I present a family of two-component, spherical, self-consistent galaxy models, in which one density distribution follows a γ_1 profile and the other a γ_2 profile [hereafter (γ_1, γ_2) models], with different total masses and "core" radii. A variable amount of (radial) orbital anisotropy is allowed in both components, following the Osipkov-Merritt parameterization. For these models, I derive analytically the necessary and sufficient conditions that the model parameters must satisfy in order to correspond to a physical system (the so-called model consistency). Moreover, the possibility of adding a black hole at the center of radially anisotropic γ models is discussed, determining analytically a lower limit of the anisotropy radius as a function of γ. The analytical phase-space distribution function for (1, 0) models is presented, together with the solution of the Jeans equations and the quantities entering the scalar virial theorem. It is proved that a globally isotropic $\gamma = 1$ component is consistent for any mass and core radius of the superimposed $\gamma = 0$ model; on the other hand, only a maximum value of the core radius is allowed for the $\gamma = 0$ model when a $\gamma = 1$ density distribution is added. The combined effects of mass concentration and orbital anisotropy are investigated, and an interesting behavior of the distribution function of the anisotropic $\gamma = 0$ component is found: there exists a region in the parameter space where a sufficient amount of anisotropy results in a consistent model, while the structurally identical but isotropic model would be inconsistent.

Subject headings: galaxies: elliptical and lenticular, cD — galaxies: halos — galaxies: kinematics and dynamics — galaxies: structure

1. INTRODUCTION

When studying a stellar dynamical model (single- or multicomponent), the fact that the Jeans equations have a physically acceptable solution is not a sufficient criterion for the validity of the model: the minimal requirement to be met by a physically acceptable model is the positivity of the phase-space distribution function (DF) of each distinct component. A model satisfying this essential requirement (which is much weaker than the stability of the model) is called a *consistent* model; moreover, when the total potential is determined by the model density components through the Poisson equation, the model is called *self-consistent*. In other words, a self-consistent model represents a physically acceptable, self-gravitating system.

Two general strategies can be used to construct a (self) consistent model or to check whether a proposed model is (self) consistent: they are commonly referred to as the "f-to-ρ" and the "ρ-to-f" approaches (Binney & Tremaine 1987, hereafter BT87). An example of the first approach is the extensive survey of self-consistent two-component spherical galaxy models carried out by Bertin, Saglia, & Stiavelli (1992), in which they assume for the stellar and dark matter components two distribution functions of the f_∞ form (and so positive by choice; Bertin & Stiavelli 1984). The main problem with this approach is that in general the spatial density is not expressible in terms of simple or at least well-known functions, and so usually only numerical investigations are feasible.

In the second approach, the density distribution is given and assumptions about the model internal dynamics are made, making the comparison with the data simpler. The difficulties inherent in the operation of recovering the DF in many cases prevent a simple consistency analysis. In particular, in order to recover the DF of spherical models with anisotropy, the Osipkov-Merritt (OM) technique (Osipkov 1979; Merritt 1985a) has been developed from the original Eddington (1916) method for isotropic systems and widely used. Examples of *numerical* application of the OM inversion to one- and two-component spherical galaxies can be found in the literature (see, e.g., Ciotti & Pellegrini 1992, hereafter CP92; Hiotelis 1994; Carollo, de Zeeuw, & van der Marel 1995a; Ciotti & Lanzoni 1997, hereafter CL97). If one is just interested in the (self) consistency of a stellar system, the previous methods obviously give "too much," i.e., give the full DF. In the OM framework, a simpler approach in order to check the (self) consistency of spherically symmetric, multicomponent models is given by the method described in CP92. This method directly uses the radial density profile of each component and of the total potential and gives necessary and sufficient conditions for the model (self) consistency, avoiding the necessity of recovering the DF itself. Moreover, since it requires only spatial differentiation and inequality checks, this method is best suited to analytical investigations.

The importance of studying multicomponent galaxy models cannot be overestimated: in fact, it is now accepted that a fraction of the mass in galaxies and clusters of galaxies is made up of a dark component, whose density distribution—albeit not well constrained by observations—differs from that of the visible one (see, e.g., Bertin et al. 1994; Carollo et al. 1995b; Buote & Canizares 1997; Gerhard et al. 1998). Moreover, there is increasing evidence for the presence of massive black holes (BHs) at the center of most (if not all) elliptical galaxies (see, e.g., Harms et al. 1994; van der Marel et al. 1997b; van der Marel,

[1] Osservatorio Astronomico di Bologna, via Ranzani 1, 40127 Bologna, Italy.
[2] Scuola Normale Superiore, Piazza dei Cavalieri 7, 56126 Pisa, Italy.

de Zeeuw, & Rix 1997a; Richstone 1998). It follows that the obvious generalization of the one-component spherical models (the dynamicists' zeroth-order approximation of real galaxies) is not only in the direction of the actively developed modeling of axisymmetric and triaxial systems (see, e.g., de Zeeuw 1996 for a review), but also in the direction of the construction of two-component analytical models and the study of their phase-space properties, a field far less developed. From this point of view, the first-order approximation of real galaxies is the construction of analytical, spherically symmetric, (self) consistent *two-component* galaxy models.

Unfortunately, few examples of two-component systems in which both the spatial density and the DF are analytically known are available, namely, the very remarkable axisymmetric Binney-Evans model (Binney 1981; Evans 1993) and the spherically symmetric two-component Hernquist model (HH models; Ciotti 1996, hereafter C96), and so it would be particularly interesting to find other members of this exclusive club. In C96 the (successful) choice of the Hernquist density distribution (Hernquist 1990, hereafter H90) as a building block for a two-component model with an analytical DF was suggested by the extremely simple (and algebraic) expression of its potential as a function of radius. Moreover, the application of the CP92 method to HH models revealed itself as both simple and fruitful, explaining many properties of the derived DF. In this line, a natural and promising extension of the HH models is obtained by considering the wider family of spherically symmetric, two-component, anisotropic (γ_1, γ_2) models. This family of models is generated by the superposition of two γ models (see eq. [7]) with different total masses, scale lengths, and slopes γ. The mass concentration and amount of mass of the two distributions are described by four free parameters, and orbital anisotropy is allowed in both components, following the OM prescription. Because the Hernquist profile is obtained from $\gamma = 1$, it will be referred to as a $\gamma = 1$ model, and so with the adopted nomenclature the HH models discussed in C96 will be called (1, 1) models. Note that an increasing interest in (γ_1, γ_2) models is seen in simulation and observational works: e.g., Pellegrini & Ciotti (1998) used (2, 1) models in their numerical simulations of hot gas flows in X-ray–emitting elliptical galaxies, and Loewenstein & White (1999) used galaxy models similar to (1, 1) models in the inner regions in order to observationally constrain the properties of dark matter halos around ellipticals.

As expected, it is not possible to find the analytical DF for (γ_1, γ_2) models in the general case, but the fact that the DF of (1, 0) models with OM anisotropy is completely expressible in an analytical way, as proved here, is still of great interest. The study of (1, 0) models is also useful for many other reasons: to provide an analytical DF for a two-component system for which the virial quantities and the analytical solution of the Jeans equation can be found explicitly; to arrange initial conditions for numerical simulations of two-component systems; to investigate the role of anisotropy and mass distribution of each component in determining the positivity of their DFs. The availability of the analytical DF for a two-component stellar system allows us to arrange with great accuracy the initial conditions for numerical simulations aimed at investigating the stability of galaxy models in the presence of dark matter halos, or with a central BH. A work on the stability of (1, 0) models is in progress (Londrillo & Ciotti, in preparation).

Strictly related to the last point above is the trend shown in numerical investigations of two-component models described in CP92, i.e., the difficulty of consistently superimposing a centrally peaked distribution on a centrally flat one. CP92 showed numerically that King (1972) or quasi-isothermal density profiles cannot be coupled to a de Vaucouleurs (1948) model, because their DFs run into negative values near the model center. On the contrary, the DF of the de Vaucouleurs component is qualitatively unaffected by the presence of centrally flat halos. From this point of view, the C96 work on (1, 1) models is complementary to the investigation of CP92; in the (1, 1) models the two density components are both centrally peaked, and their DF is positive (in the isotropic case) for all the possible choices of halo and galaxy masses and concentrations.

The implications of these findings have been not explored sufficiently. One could speculate that in the presence of a centrally peaked dark matter halo, King-like elliptical galaxies should be relatively rare, or that a galaxy with a central power-law density profile cannot have a dark halo that is too flat in the center. In fact, observations of the central surface brightness profiles of elliptical galaxies (see, e.g., Ferrarese et al. 1994; Jaffe et al. 1994; Møller, Stiavelli, & Zeilinger 1995; Lauer et al. 1995; Kormendy et al. 1995; Byun et al. 1996) and bulges of spirals (Carollo & Stiavelli 1998), as well as high-resolution numerical simulations of dark matter halo formation (see, e.g., Dubinski & Carlberg 1991; White 1996; Navarro, Frenk, & White 1997) seem to point in this direction.

In this paper, I further explore the trend that emerged in CP92 and in C96, determining the limits imposed by phase-space constraints (i.e., the DF positivity) on the parameters describing the (γ_1, γ_2) models and γ models with a central BH [hereafter (γ, BH) models]. I focus on the (1, 0) models, in which one component is centrally peaked ($\gamma = 1$ density profile) and the other has a flatter core ($\gamma = 0$ density profile). With the aid of the derived analytical DFs, more stringent conclusions are then reached.

In § 2, I briefly review the technique developed in CP92 and applied in C96 to (1, 1) models, and I formulate it in a way suitable for its application to the present problem. In § 3 the (γ_1, γ_2) models are introduced, as well as the CP92 method used to discuss the limits imposed on their parameters by requiring the positivity of the DF of the two components. In § 4 the DFs for the two components of (1, 0) models are derived explicitly, and in § 5 the exact boundaries of the region of consistency in the parameter space are obtained and compared to those given in § 3. Finally, in § 6 the main results are summarized. In the Appendices, the analytical expressions for the velocity dispersion profiles of both the (1, 0) model components and the virial quantities useful in applications are derived in the general OM case.

2. THE CONSISTENCY OF MULTICOMPONENT SYSTEMS

As outlined in the Introduction, a stellar system described as a sum of different density components ρ_k is called consistent if *each* f_k is nonnegative over all the accessible phase space; a consistent, self-gravitating system is called self-consistent. The technique developed in CP92 permits us to check whether the DF of a multicomponent spherical system, in which the orbital anisotropy of each component is modeled according to the OM parameterization, is positive, *without* calculating it effectively.

In the OM formulation, the radially anisotropic case is obtained as a consequence of assuming $f = f(Q)$, with

$$Q = \mathscr{E} - \frac{L^2}{2r_a^2}\,, \tag{1}$$

where $\mathscr{E}$ and L are the relative energy and the angular momentum modulus per unit mass, respectively, r_a is the so-called *anisotropy radius*, and $f(Q) = 0$ for $Q \leq 0$. With this assumption, the models are characterized by radial anisotropy increasing with galactic radius, and in the limit as $r_a \to \infty$, the velocity dispersion tensor becomes globally isotropic. For a multi-component spherical system, the simple relation between energy and angular momentum prescribed by equation (1) allows us to express the DF of the kth component as

$$f_k(Q_k) = \frac{1}{\sqrt{8}\pi^2}\frac{d}{dQ_k}\int_0^{Q_k}\frac{d\varrho_k}{d\Psi_T}\frac{d\Psi_T}{\sqrt{Q_k - \Psi_T}} = \frac{1}{\sqrt{8}\pi^2}\int_0^{Q_k}\frac{d^2\varrho_k}{d\Psi_T^2}\frac{d\Psi_T}{\sqrt{Q_k - \Psi_T}}\,, \tag{2}$$

where

$$\varrho_k(r) = \left(1 + \frac{r^2}{r_{ak}^2}\right)\rho_k(r)\,, \tag{3}$$

$\Psi_T(r) = \sum_k \Psi_k(r)$ is the total relative potential, $Q_k = \mathscr{E} - L^2/2r_{ak}^2$, and $0 \leq Q_k \leq \Psi_T(0)$. The second equivalence in equation (2) holds for untruncated systems with finite total mass, such as the models discussed here (see, e.g., BT87, p. 240). In C96, the original CP92 technique was applied to (1, 1) models using the relative potential Ψ_k of the investigated component as the independent variable, but here the radius r is found to be a more convenient variable. Therefore, we have now

THEOREM: *A* necessary condition (NC) *for the nonnegativity of* f_k *is*

$$\frac{d\varrho_k(r)}{dr} \leq 0\,, \qquad 0 \leq r \leq \infty\,. \tag{4}$$

If the NC is satisfied, a strong sufficient condition (SSC) *for the nonnegativity of* f_k *is*

$$\frac{d}{dr}\left[\frac{d\varrho_k(r)}{dr}\frac{r^2\sqrt{\Psi_T(r)}}{M_T(r)}\right] \geq 0\,, \qquad 0 \leq r \leq \infty\,. \tag{5}$$

Finally, a weak sufficient condition (WSC)[3] *for the nonnegativity of* f_k *is*

$$\frac{d}{dr}\left[\frac{d\varrho_k(r)}{dr}\frac{r^2}{M_T(r)}\right] \geq 0\,, \qquad 0 \leq r \leq \infty\,. \tag{6}$$

Proof. See CP92 and C96.

Some considerations follow from the above conditions. The first is that the violation of the NC (eq. [4]) is connected only to the radial behavior of ρ_k and the value of r_{ak}, and so this condition applies independently of any other component added to the model. Obviously, the condition imposed by equation (4) is only necessary, so f_k can be negative (and so the k component will be inconsistent) even for values of model parameters allowed by the NC. This is due to the radial behavior of the integrand in equation (2), which depends not only on the particular ρ_k and r_{ak}, but also on the total potential. To summarize: a model failing the NC is *certainly inconsistent*; a model satisfying the NC *can be consistent*. The second consideration is that a model satisfying the WSC (or the more restrictive SSC) is *certainly* consistent, while a model failing the WSC (SSC) *can be consistent*, because of the sufficiency of the conditions given by equations (5) and (6). As a consequence, the consistency of a model satisfying the NC and failing the WSC (or the SSC) can be proved only by direct inspection of its DF. For example, if one find that for $r_{ak} \leq r_{ak}(\mathrm{NC})$ the model is inconsistent (i.e., eq. [4] is not verified), while for $r_{ak} \geq r_{ak}(\mathrm{WSC}) \geq r_{ak}(\mathrm{SSC})$ the model is consistent (i.e., eqs. [5] or [6] are verified), this means that the true critical anisotropy radius (r_{akc}) for that model must satisfy the relation $r_{ak}(\mathrm{NC}) \leq r_{akc} \leq r_{ak}(\mathrm{SSC}) \leq r_{ak}(\mathrm{WSC})$. In this case, the limitations on r_{ak} obtained from WSC or SSC are upper bounds on the lower limit r_{akc}, for consistency. Obviously, the situation can be more complicated (see eqs. [38] and [39] and the following discussion).

In the next section, after presenting the (γ_1, γ_2) models, the analytical constraints on r_a for the consistency of the one-component OM anisotropic γ models are derived, together with a general result on the consistency of two-component isotropic (γ_1, γ_2) models. Successively more specific results for the isotropic (1,0) models are proved. Finally, a limitation on r_a for the OM anisotropic (γ, BH) models is explicitly derived as a function of γ.

3. THE (γ_1, γ_2) MODELS

Both density distributions of the (γ_1, γ_2) models belong to the widely explored family of the so-called γ models (Dehnen 1993, hereafter D93; Carollo 1993; Tremaine et al. 1994):

$$\rho(r) = \frac{3-\gamma}{4\pi}\frac{Mr_c}{r^\gamma(r_c + r)^{4-\gamma}}\,, \qquad M(r) = M\left(\frac{r}{r_c + r}\right)^{3-\gamma}\,, \qquad 0 \leq \gamma < 3\,, \tag{7}$$

[3] The WSC is better suited to analytical investigations than the SSC, because of the absence of the weighting square root of the total potential.

where M is the total mass and r_c is a characteristic scale length. The corresponding relative potential is given by

$$\Psi(r) = \frac{GM}{r_c(2-\gamma)}\left[1-\left(\frac{r}{r+r_c}\right)^{2-\gamma}\right],$$
$$\Psi(r) = \frac{GM}{r_c}\ln\left(\frac{r+r_c}{r}\right), \tag{8}$$

where the second expression holds for $\gamma = 2$. In the following discussion, the mass $M = M_{\gamma_1}$ and the characteristic scale length $r_c = r_{c1}$ of the γ_1 model will be adopted as normalization constants, so that from equation (7) it follows that $\rho_{\gamma_1}(r) = \rho_N \tilde{\rho}_{\gamma_1}(s)$ and $\rho_{\gamma_2}(r) = \rho_N \mu \tilde{\rho}_{\gamma_2}(s, \beta)$, where $s = r/r_{c1}$, $\rho_N = M_{\gamma_1}/r_{c1}^3$, $\mu = M_{\gamma_2}/M_{\gamma_1}$, and $r_{c2} = \beta r_{c1}$. The fundamental ingredient in recovering the DF is the total potential $\Psi_T = \Psi_{\gamma_1} + \Psi_{\gamma_2}$, where from equation (8) $\Psi_{\gamma_1}(r) = \Psi_N \tilde{\Psi}_{\gamma_1}(s)$, $\Psi_{\gamma_2}(r) = \Psi_N \mu \tilde{\Psi}_{\gamma_2}(s, \beta)$, and $\Psi_N = GM_{\gamma_1}/r_{c1}$. With this choice, the (γ_1, γ_2) models are structurally determined by fixing the four independent parameters (M_{γ_1}, r_{c1}, μ, and β), with the obvious condition that $\mu \geq 0$ and $\beta \geq 0$.

For future reference, I give here the explicit expressions of the density and the potential for the (1, 0) models, for which $(M_{\gamma_1}, r_{c1}, \rho_{\gamma_1}, \Psi_{\gamma_1}) = (M_1, r_1, \rho_1, \Psi_1)$ and $(M_{\gamma_2}, r_{c2}, \rho_{\gamma_2}, \Psi_{\gamma_2}) = (M_0, r_0, \rho_0, \Psi_0)$:

$$\rho_1(r) = \rho_N \tilde{\rho}_1(s) = \frac{\rho_N}{2\pi}\frac{1}{s(1+s)^3} \tag{9}$$

and

$$\rho_0(r) = \rho_N \mu \tilde{\rho}_0(s) = \mu \frac{3\rho_N}{4\pi}\frac{\beta}{(\beta+s)^4}, \tag{10}$$

where $s = r/r_1$, $\rho_N = M_1/r_1^3$, $M_0 = \mu M_1$, and $r_0 = \beta r_1$; moreover,

$$\Psi_1(r) = \Psi_N \tilde{\Psi}_1(s) = \frac{\Psi_N}{1+s}, \tag{11}$$

$$\Psi_0(r) = \Psi_N \mu \tilde{\Psi}_0(s) = \Psi_N \mu \frac{\beta+2s}{2(\beta+s)^2}, \tag{12}$$

with $\Psi_N = GM_1/r_1$.

3.1. *The Necessary and Sufficient Conditions for the γ Models*

Here I study first the NC for the general case of the anisotropic one-component γ models, in order to determine analytically a *critical* anisotropy radius such that a higher degree of radial OM anisotropy (i.e., a smaller anisotropy radius) produces a negative DF for some permitted value of Q, no matter what kind of halo density distribution is added. The unit mass and unit length are the total mass M and the scale length r_c of the model, with $s_a = r_a/r_c$.

As shown in Appendix A (eqs. [A1] and [A2]), for $2 \leq \gamma < 3$ the NC is satisfied for $s_a \geq 0$, i.e., the possibility that γ models with $\gamma \geq 2$ are assembled using only radial orbits is left open by the NC. On the other hand, for $0 \leq \gamma < 2$ the NC requires

$$s_a \geq s_M \sqrt{\frac{2-\gamma-2s_M}{\gamma+4s_M}}, \tag{13}$$

where $s_M = s_M(\gamma)$ is given by equation (A2). In this case the NC *proves* that γ models with $0 \leq \gamma < 2$ cannot sustain radial orbits only. In Figure 1 the lower bound for the anisotropy radius as a function of γ derived from the NC is shown. From the discussion in § 2, it follows that all γ models (one- or multicomponent) in the nearly triangular region under the solid curve are inconsistent.

The WSC can be treated analytically for the one-component γ models, as shown in Appendix A (eqs. [A3]–[A6]), and we obtain the following limits on s_a:

$$s_a \geq s_M^{3/2} \sqrt{\frac{3-\gamma-s_M}{6s_M^2+2(1+\gamma)s_M+\gamma}}, \tag{14}$$

where $s_M = s_M(\gamma)$ is given by equations (A4)–(A6). As discussed in § 2, the right-hand side of equation (14) (represented in Fig. 1 by the dotted line) is an upper limit on the lower bound for the critical anisotropy radius as a function of γ: all one-component γ models in the region above the dotted line are consistent.

A stronger limitation on r_a is obtained using the SSC, but unfortunately this condition for a generic γ results in a transcendental equation that cannot be solved explicitly. However, as shown in Appendix A, for the three values $\gamma = (0, 1, 3)$ the solution can be derived explicitly. For $\gamma = 0$,

$$s_a \geq s_M \sqrt{\frac{3(1+2s_M-s_M^2)}{14s_M^2+10s_M+2}} \simeq 0.501, \tag{15}$$

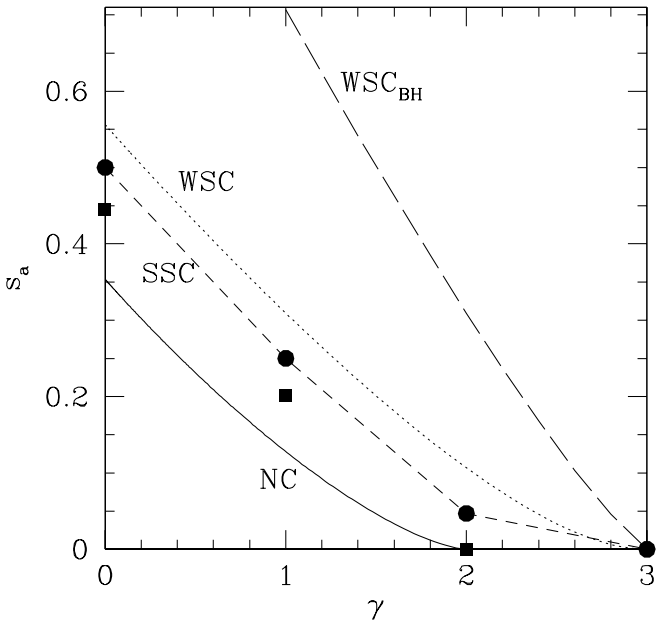

FIG. 1.—Limits on the anisotropy radius for the consistency of the one-component γ models as a function of γ. The solid line represents the lower limit as determined by the NC, and the dotted line the upper limit as given by the WSC. For $\gamma = (0, 1, 2, 3)$, the filled circles connected by the dashed line represent the upper limits obtained using the SSC, while the true limits derived from the DFs are shown by filled squares. The long-dashed line represents the limit on the anisotropy radius in the presence of a dominant central BH.

where $s_M = s_M(0)$ is given by equation (A8). For $\gamma = 1$, equation (A9) shows that

$$s_a \geq s_M^{3/2} \sqrt{\frac{3(3 - 2s_M)}{28s_M^2 + 17s_M + 4}} \simeq 0.250 , \tag{16}$$

where $s_M = s_M(1)$ is given by equations (A10) and (A11). The numerical application of the SSC to the $\gamma = 2$ model (Jaffe 1983) gives $s_a \gtrsim 0.047$. Finally, the case of $\gamma = 3$ is trivial, and the SSC reduces to $s_a \geq 0$. These four values are represented in Figure 1 by filled circles; all one-component γ models in the region above the dashed line are consistent. Note how the SSC improves the estimate of the lower bound of r_a with respect to the WSC.

As already pointed out in § 2, the true critical value of s_a for any one-component γ model is between the NC and the SSC curves. For the $\gamma = 0$ and $\gamma = 1$ models these values, determined directly from their DFs (§§ B1 and B2 in Appendix B), are $\simeq 0.445$ and $\simeq 0.202$, respectively. Merritt (1985b) derived the analytical DF for a totally radial Jaffe model (the $\gamma = 2$ case); its positivity implies that in this case the true lower limit on s_a is zero. In Figure 1 these three values are represented by filled squares, and in Table 1 all the previous results for the specific cases $\gamma = (0, 1, 2, 3)$ are summarized; note how the more the model is concentrated, the more radial anisotropy can be supported. The true critical r_a value for the OM anisotropic one-component γ models as a function of γ is numerically known (see Fig. 1 in Carollo et al. 1995a).

3.2. *Sufficient Conditions for Isotropic* (γ_1, γ_2) *Models*

In order to proceed further with this analytical discussion, and to allow for the presence of a "halo" component, we will use the WSC rather than the more complicated SSC. The following three results are proven analytically in this section:

1. In the case of globally isotropic two-component (γ_1, γ_2) models with $1 \leq \gamma_1 < 3$ and $0 \leq \gamma_2 \leq \gamma_1$, the DF of the more peaked component γ_1 is positive over all the phase space for all values of $(\mu, \beta) = (M_{\gamma 1}/M_{\gamma 2}, r_{c2}/r_{c1})$. As a consequence, the $\gamma = 1$ component of (1, 0) models is consistent for all values of the parameters (μ, β).
2. In the case of globally isotropic (1, 0) models, the WSC applied to the $\gamma = 0$ density distribution suggests the existence of a lower limit of $\mu = M_0/M_1$ as a function of $\beta = r_0/r_1$. In particular, for $\beta \leq 5/2$, i.e., when the $\gamma = 0$ component is sufficiently concentrated, all values of μ can be accepted. Using the analytical DF, the existence of this lower limit will be proved in § 5.

TABLE 1

CRITICAL VALUES OF $s_a = r_a/r_c$ FOR γ MODELS

γ	NC	True[a]	SSC	WSC	WSC$_{BH}$[b]
0.....	0.354	0.445	0.501	0.556	...
1.....	0.128	0.202	0.250	0.310	0.707
2.....	0.000	0.000	0.047	0.107	0.309
3.....	0.000	0.000	0.000	0.000	0.000

[a] Obtained from the model DF.
[b] Case with a dominant central BH.

3. In the case of anisotropic γ models with a BH at their center, it is possible to determine analytically a lower limit on r_a as a function of γ using the WSC.

The proof of the first result is conceptually straightforward but algebraically cumbersome. In Appendix A (eqs. [A12] and [A13]) it is proved that under the hypothesis assumed in point 1 above, equation (6) is verified for all choices of (μ, β). I note explicitly that this result contains as a particular case the fact (already proved in C96) that globally isotropic (1, 1) models can be self–consistently assembled for any choice of (μ, β). From this general result it also follows that, e.g., the same is true for isotropic Jaffe + Jaffe models ($\gamma_1 = \gamma_2 = 2$). Finally, considering that for $r_c \to 0$ the potential of γ models becomes that of a point mass (see eq. [8]), the previous result means that a BH of any mass can be added at the center of a globally isotropic γ model when $1 \leq \gamma < 3$. A different analysis, based on a series expansion of the integral representation of the DF for isotropic γ models, shows that the true limit on γ in order to allow for the presence of a BH of any mass at the models center is $\gamma > \frac{1}{2}$ (Tremaine et al. 1994).

The result stated in point 2 above is proved in Appendix A (eq. [A14]). For equation (6) to be satisfied for the isotropic $\gamma = 0$ component of (1, 0) models, a sufficient condition for the consistency of this component is

$$\mu \geq (2\beta - 5)\beta^2 \, . \tag{17}$$

This requirement can be interpreted in two different ways. The first is that, having fixed the ratio $\beta = r_0/r_1$, only for sufficiently high mass ratios $\mu = M_0/M_1$ can the $\gamma = 0$ component "dilute" the effect of the central cusp of the $\gamma = 1$ model on the total potential and be consistent. More specifically, when $\beta < 5/2$ (i.e., when the $\gamma = 0$ density distribution is sufficiently concentrated), even a vanishing mass M_0 ($\mu \to 0$) can be accepted, while for large β only very large μ are allowed. From another point of view, equation (17) tells us that having fixed μ, β cannot be arbitrarily large, but in some sense the concentration of the $\gamma = 0$ component must adapt to the density distribution of the $\gamma = 1$ component. The effect of the concentration is much more important than the amount of mass; in fact, $\beta \lesssim (\mu/2)^{1/3}$. This means that even considerably increasing the mass ratio, the maximum value of r_0 allowed for the $\gamma = 0$ model grows only as the *cube* root of μ. The limitation $\beta \leq 5/2$ is only a *sufficient* condition for the consistency of a $\gamma = 0$ model coupled with a dominant $\gamma = 1$; a larger critical value for β is expected from direct inspection of the DF when $\mu \to 0$ (see § 5).

The result presented in point 3 above can be interpreted as an extension of the radially anisotropic case of the analysis performed by Tremaine et al. (1994), and is proved in Appendix A by showing that the WSC applied to the anisotropic (γ, BH) models with $1 \leq \gamma < 3$ can be analytically discussed in the special case of a *dominant* BH, i.e., assuming in equation (6) $M_T = M_{\rm BH}$ (and so $\Psi_T = GM_{\rm BH}/r$). Unfortunately, in the nonasymptotic case the equation to be discussed is transcendental, and no analytical discussion can be carried out. At first, the assumption of a dominant BH could appear as a very rough approximation of reality, but this is not true: the constraint derived can be used as a safe limitation when constructing models containing BHs of realistic mass at their centers. As shown in Appendix A (eq. [A15]), for $1 \leq \gamma < 3$,

$$s_a \geq s_M \sqrt{\frac{(3-\gamma)(\gamma-2) + 4(3-\gamma)s_M - 2s_M^2}{12s_M^2 + 8(\gamma-1)s_M + \gamma(\gamma-1)}} \, , \tag{18}$$

where $s_M = s_M(\gamma)$ is obtained by solving a fourth-degree algebraic equation. In Figure 1, the long-dashed line represents the lower bound for s_a as determined by the previous equation, while the explicit values for $\gamma = (1, 2, 3)$ are given in Table 1. In particular, the critical value for the $\gamma = 1$ model was already derived as a limiting case of a (nonasymptotic) formula given in C96 (eq. [15]).

4. THE DF OF (1, 0) MODELS

We can now proceed to the explicit recovery of the DF of the (1, 0) models. Just as for the density and the potential, it is also useful for the DF to work with dimensionless functions: the two components of the DF are of the form $f = f_N \tilde{f}(\mu, \beta; \tilde{Q})$, with $f_N = \rho_N \Psi_N^{-3/2}$ and $0 \leq \tilde{Q} = Q/\Psi_N \leq \tilde{\Psi}_1(0) + \mu\tilde{\Psi}_0(0)$. The easiest way to compute each DF is to use the first of the identities in equation (2). For the evaluation of the integral, one would be tempted to obtain $\varrho(\Psi_T)$, eliminating the radius from the modified density and the total potential; formally, this can be done, but the resulting expression for the radial coordinate involves a quadratic irrationality that, after insertion in equations (3), (9), and (10), produces an intractable expression. Here I follow another approach: instead of eliminating the radius, the integration variable is changed from the total potential to the radius itself. This is equivalent to a remapping of the domain of definition of each f from the range of variation of Ψ_T to the range of variation of r and leads us to introduce the dimensionless radius v, using equations (11) and (12):

$$\tilde{Q} = \frac{1}{1+v} + \mu \frac{\beta + 2v}{2(\beta + v)^2} \, , \qquad 0 \leq v \leq \infty \, . \tag{19}$$

As shown in Appendix B (eqs. [B1] and [B2]), with this change of variable and after normalization to the dimensional scales of the Hernquist density distribution, the DF for the $\gamma = 1$ and $\gamma = 0$ components can be formally written as

$$f(Q) = f_i(Q) + \frac{f_a(Q)}{s_a^2} = \frac{f_N}{\sqrt{8}\pi^2} \left(\frac{d\tilde{Q}}{dv}\right)^{-1} \frac{d}{dv}\left[\tilde{F}_i(v) + \frac{\tilde{F}_a(v)}{s_a^2}\right] , \qquad v = v(\tilde{Q}) \, , \tag{20}$$

where $s_a = r_a/r_1$ and the subscripts refer to the isotropic and anisotropic parts of the DF, respectively. Following the procedure, $f(Q)$ results from the elimination of v between equations (19) and (20). In the general case, i.e., for any choice of (μ, β, s_a), $f(Q)$ (and the so called *differential energy distribution* for each component as well; see, e.g., BT87, p. 242) can be recovered analytically (see eq. [B3] for a proof of this fact). It is thus shown that in addition to the (1, 1) models, the (1, 0)

models are a class of two-component stellar systems in which the spatial density distributions, the solution of the Jeans equations (see Appendix C), and the phase-space distribution functions can all be explicitly found. Unfortunately, the DF of the (1, 0) models results in a combination of elliptic functions that is even more complicated than the DF of the (1, 1) models, and this limits their applicability to special problems in which the DF is required to be known with arbitrary precision or to be formally manipulated.

Here I present only the DFs for the two density distributions obtained under the assumption of a dominant "halo" component; I derive the DF for a $\gamma = 1$ model with a dominant $\gamma = 0$ halo ($\mu \to \infty$) and for a $\gamma = 0$ model with a dominant $\gamma = 1$ halo ($\mu \to 0$). Technically, this reduces to the assumption that the total potential is the potential of the halo component only. Even though it is a limiting case, the study of *halo-dominated* models is interesting for several different reasons: (1) the formulae—expressible using elementary functions—are much simpler than in the general case, and can be studied very easily, making the effect of the halo component on the DF clearer; (2) the halo-dominated case is the one that differs most from the case of the corresponding one-component model, and so the differences are more evident; and (3) all the intermediate cases fall between the one-component model and the halo-dominated one. A comparison with more realistic values of the halo masses is postponed to § 5.

In the following paragraphs, the two DFs will be compared with those of the corresponding one-component $\gamma = 1$ and $\gamma = 0$ models, and the exact phase-space constraints will be derived and compared with those obtained using the NC, WSC, and SSC in § 3.

4.1. *The $\gamma = 1$ Model Plus a $\gamma = 0$ Dominant Halo*

The explicit expression for the DF of the $\gamma = 1$ model with an arbitrary degree of OM orbital anisotropy immersed in a dominant $\gamma = 0$ halo is derived here. Formally, this case corresponds to the assumption of $\mu \to \infty$ in the total potential, i.e., $\Psi_T = \Psi_0$, and so in equations (19) and (20)

$$\tilde{Q} = \mu \frac{\beta + 2v}{2(\beta + v)^2}, \qquad \left(\frac{d\tilde{Q}}{dv}\right)^{-1} = -\frac{(\beta + v)^3}{\mu v}. \tag{21}$$

After differentiation inside the integral in equation (B2) with $\tilde{\varrho}$ given by equations (3) and (9), and after a partial fraction decomposition of the rational part of the integrand, one obtains

$$\tilde{F}_i(v) = \frac{\beta + v}{\pi\sqrt{2\mu}\sqrt{\beta + 2v}} [H_1^0 + \beta H_2^0 - H_1^1 - (1 + \beta)H_2^1 - (1 + 2\beta)H_3^1 - 3(\beta - 1)H_4^1] \tag{22}$$

and

$$\tilde{F}_a(v) = \frac{\beta + v}{\pi\sqrt{2\mu}\sqrt{\beta + 2v}} [2H_2^1 - (5 - 2\beta)H_3^1 - 3(\beta - 1)H_4^1]. \tag{23}$$

The H functions depend on β and v, and are defined as

$$H_n^z(\xi) = \frac{2}{(v + \lambda)^n} \int_0^\infty \frac{dx}{\sqrt{1 + x^2}(x^2 + \xi)^n}, \tag{24}$$

where

$$\xi = \frac{v + z}{v + \lambda} \qquad \text{and} \qquad \lambda = \frac{\beta v}{\beta + 2v}. \tag{25}$$

When $\xi = 1$ and $n \geq 1$,

$$H_n^z(1) = \frac{\sqrt{\pi}\,\Gamma(n)}{\Gamma(n - 1/2)(v + \lambda)^n}, \tag{26}$$

where Γ is the complete gamma function. When $\xi \neq 1$, the recursion formula

$$H_{n+1}^z(\xi) = -\frac{1}{n(v + \lambda)} \frac{dH_n^z(\xi)}{d\xi} = \frac{(-1)^n}{n!(v + \lambda)^n} \frac{d^n H_1^z(\xi)}{d\xi^n} \tag{27}$$

holds, and so the explicit evaluation of $H_1^z(\xi)$ suffices:

$$H_1^z(\xi) = \frac{2}{v + \lambda} \begin{cases} \dfrac{\cos^{-1}\sqrt{\xi}}{\sqrt{\xi(1 - \xi)}}, & \text{if } 0 \leq \xi < 1, \\ \dfrac{\cosh^{-1}\sqrt{\xi}}{\sqrt{\xi(\xi - 1)}}, & \text{if } \xi > 1. \end{cases} \tag{28}$$

In order to distinguish between the two cases $\xi > 1$ and $0 \leq \xi < 1$, a careful discussion is needed. From equation (25), the value $z = 0$ corresponds to $\xi = v/(v + \lambda) < 1$ for all (v, β), and so the first case of equation (28) must be used for the evaluation of all H_n^0 functions. More complicated is the case of $z = 1$, when $\xi = (v + 1)/(v + \lambda)$; note that for $\beta \geq 0$, λ is a monotonically increasing function of v, with $\lambda = 0$ for $v = 0$ and $\lambda \to \beta/2$ for $v \to \infty$. As a consequence, it follows that for all v, $0 < \beta \leq 2$

implies $\xi > 1$. When instead $\beta > 2$, there is $v_{cr} = \beta/(\beta - 2)$, so that $v < v_{cr}$ implies $\xi > 1$, $v = v_{cr}$ implies $\xi = 1$, and $v > v_{cr}$ implies $\xi < 1$. This completes the derivation of the DF for the $\gamma = 1$ component.

In Figure 2 the comparison with the DF of the one-component $\gamma = 1$ model (*solid line*) is given in the case of global isotropy and for a specific value of the anisotropy radius. Such a DF was given in H90 as a function of $\tilde{Q}$, but for consistency with the present work it is derived in Appendix B as a function of v (eqs. [B4]–[B6]). The formulae derived in this paragraph have been tested for many values of β and r_a using a code that numerically recovers the DF for spherically symmetric multicomponent galaxy models with OM anisotropy. We obtained extremely good agreement; in all cases the maximum differences between the analytical and numerical DFs are much less than 1%.

In the upper panel of Figure 2 the isotropic case is presented. Note that for $\beta > 1$ the DF is more peaked than for the one-component $\gamma = 1$ model, and the opposite holds when $\beta < 1$: this behavior has already been found in the isotropic (1, 1) models (C96, Fig. 2). In the lower panel the anisotropic case is shown when $s_a = 0.26$, near the consistency limit for the one-component $\gamma = 1$ model (see § 3.1). The main effect of anisotropy, as already found for (1, 1) models and $R^{1/m}$ models (CL97), is the appearance in the DF of a depression well outside the galaxy center. Decreasing the anisotropy radius, the depression deepens, running finally into negative values for a critical value of s_a (dependent on β) and making the model inconsistent. Again, as already found for (1, 1) models, this effect is stronger for smaller β values, i.e., a very concentrated halo makes the DF more sensitive to the effects of anisotropy, while the opposite is true for halos more diffuse than the $\gamma = 1$ density distribution.

4.2. *The $\gamma = 0$ Model Plus a $\gamma = 1$ Dominant Halo*

The explicit expression for the DF of a $\gamma = 0$ model with an arbitrary degree of OM orbital anisotropy immersed in a dominant Hernquist halo is derived here. Formally, this case corresponds to the assumption of $\mu \to 0$ in the total potential, i.e., $\Psi_T = \Psi_1$, and so in equations (19) and (20),

$$\tilde{Q} = \frac{1}{1 + v}, \qquad \left(\frac{d\tilde{Q}}{dv}\right)^{-1} = -(1 + v)^2 . \tag{29}$$

After differentiation inside the integral in equation (B2) with $\tilde{\varrho}$ given by equations (3) and (10), and after a partial fraction decomposition of the rational part of the integrand, one obtains

$$\tilde{F}_i(v) = \frac{3\mu\beta\sqrt{1 + v}}{4\pi} 4G_5 \tag{30}$$

and

$$\tilde{F}_a(v) = \frac{3\mu\beta\sqrt{1 + v}}{4\pi}(4\beta^2 G_5 - 6\beta G_4 + 2G_3) , \tag{31}$$

where

$$G_n(\beta, v) = \int_v^\infty \sqrt{\frac{s + 1}{s - v}} \frac{ds}{(\beta + s)^n} . \tag{32}$$

When $\beta = 1$ and $n \geq 2$,

$$G_n(1, v) = \frac{\sqrt{\pi}\,\Gamma(n - 1)}{\Gamma(n - 1/2)(1 + v)^{n-1}} . \tag{33}$$

When $\beta \neq 1$ and $n \geq 2$, the recursion formula

$$G_{n+1}(\beta, v) = -\frac{1}{n}\frac{dG_n(\beta, v)}{d\beta} = \frac{(-1)^{n-1}}{n!}\frac{d^{n-1}G_2(\beta, v)}{d\beta^{n-1}} \tag{34}$$

holds, and so the explicit evaluation of G_2 suffices:

$$G_2(\beta, v) = \frac{1}{\beta + v} + \frac{1 + v}{(\beta + v)^{3/2}} \begin{cases} \dfrac{1}{\sqrt{1 - \beta}} \tan^{-1}\sqrt{\dfrac{1 - \beta}{\beta + v}}, & \text{if } 0 \leq \beta < 1 , \\ \dfrac{1}{\sqrt{\beta - 1}} \tanh^{-1}\sqrt{\dfrac{\beta - 1}{\beta + v}}, & \text{if } \beta > 1 . \end{cases} \tag{35}$$

In Figure 3 the comparison with the DF of the one-component $\gamma = 0$ model (*solid line*) is shown for the case of global isotropy and for a specific value of the anisotropy radius. Such a DF was given in D93 as a function of $\tilde{Q}$, but for consistency with the present work it is derived in Appendix B as a function of v (eqs. [B7]–[B9]). As in the previous case, the derived formulae have been successfully tested for many values of β and r_a by comparison with the numerically derived DFs, obtaining maximum differences of less than 1% in any case.

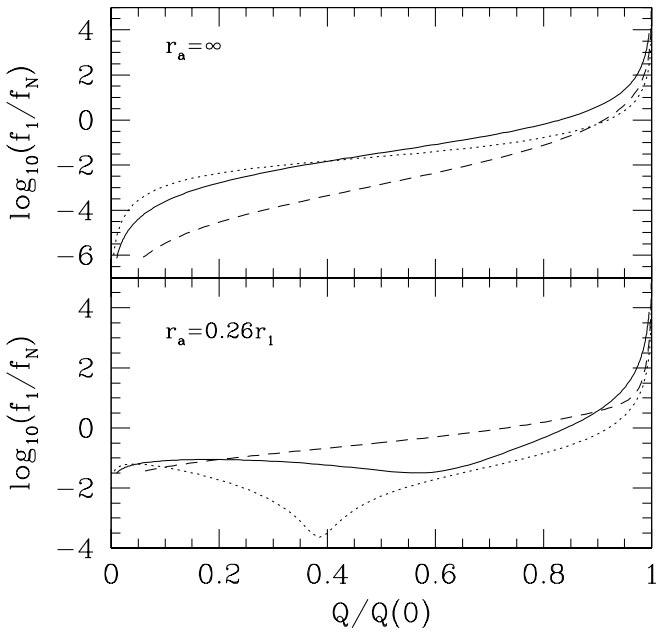

FIG. 2.—Dimensionless DF f_1/f_N for the one-component $\gamma = 1$ model [*solid line*, $Q(0) = \Psi_1(0)$ on the abscissae], and the case of a dominant $\gamma = 0$ halo [$\lim_{\mu\to\infty} \mu^{3/2} f_1/f_N$, $Q(0) = \Psi_0(0)$ on the abscissae] for $\beta = 0.2$ (*dotted line*) and $\beta = 3$ (*dashed line*). The upper panel shows the globally isotropic case, while in the lower panel the anisotropy radius is fixed at $r_a = 0.26 r_1$. The normalization constant is $f_N = G^{-3/2} M_1^{-1/2} r_1^{-3/2}$.

In the upper panel of Figure 3 the isotropic case is presented. Note that for $\beta < 1$ the DF is more peaked than for the one-component $\gamma = 0$ model, and the opposite holds when $\beta < 1$.[4] This behavior is similar to that found in the previous section. In the lower panel the anisotropic case is shown when $r_a = 0.65 r_0$, near the consistency limit for the one-component $\gamma = 0$ model (see § 3.1). As for the $\gamma = 1$ component, the main effect of anisotropy is the appearance in the DF of a depression well outside the galaxy center, and again the depression becomes deeper and deeper, decreasing the anisotropy radius. Finally, as in the previous case, the effect of anisotropy is found to be more important when the halo concentration increases.

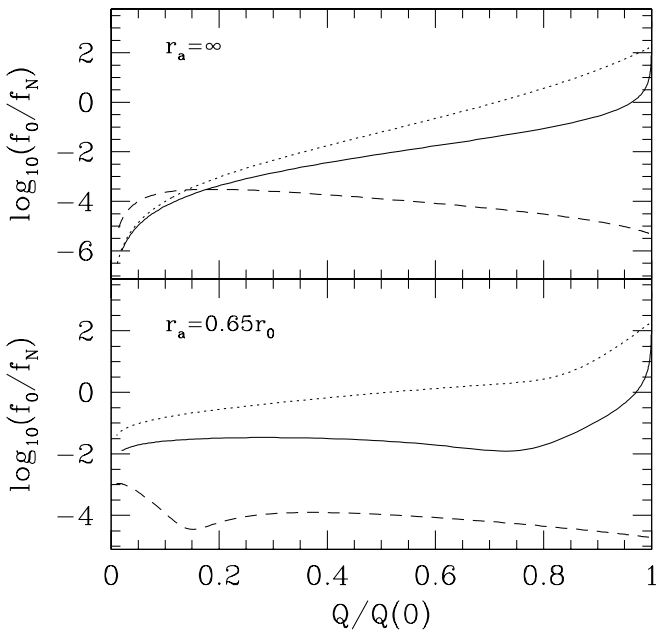

FIG. 3.—Dimensionless DF f_0/f_N for the one-component $\gamma = 0$ model [*solid line*, $Q(0) = \Psi_0(0)$ on the abscissae, $f_N = G^{-3/2} M_0^{-1/2} r_0^{-3/2}$], and the case of a dominant $\gamma = 1$ halo [$\lim_{\mu\to 0} \mu^{-1} f_0/f_N$, $Q(0) = \Psi_1(0)$ on the abscissae, $f_N = G^{-3/2} M_1^{-1/2} r_1^{-3/2}$] for $\beta = 0.2$ (*dotted line*) and $\beta = 5$ (*dashed line*). The upper panel shows the globally isotropic case, while in the lower panel the anisotropy radius is fixed at $r_a = 0.65 r_0$.

[4] Having defined $\beta = r_0/r_1$, at variance with the discussion in § 4.1, a more diffuse $\gamma = 1$ component corresponds to $\beta < 1$ and vice versa.

5. CONSISTENCY OF (1, 0) MODELS

We move now to comment on the main similarities and differences between the DFs of the two components of the (1, 0) models, especially considering the role of concentration and orbital anisotropy in determining their consistency. For simplicity, the discussion is restricted to the halo-dominated cases.

The first important point addressed by using the DFs is the study of the effect of halo concentration in determining the consistency of the two (1, 0) model components in the case of *global isotropy*. The effect of the $\gamma = 0$ halo concentration on the consistency of the globally isotropic $\gamma = 1$ component can be derived by the direct inspection of the DF and confirms the analytical prediction obtained using the WSC in § 3.1. In fact, it is found that the globally isotropic $\gamma = 1$ component is consistent independent of the concentration and total mass of the superimposed $\gamma = 0$ halo: *only the anisotropic* $\gamma = 1$ component in (1, 0) models can be unphysical due to the presence of the $\gamma = 0$ density distribution.

For the globally isotropic $\gamma = 0$ component with a dominant $\gamma = 1$ halo, the situation is more complicated because, in accordance with the analysis presented in § 3.2, its DF may become negative in the case of a high concentration of the external $\gamma = 1$ component. In fact, the DF becomes negative for $\mathscr{E} \to \Psi_1(0)$ when $\beta \gtrsim 5.233$, a larger value than the more conservative one (5/2) derived using the WSC. A closer look at this behavior, and a comparison with the qualitatively different behavior exhibited by the DF of the $\gamma = 1$ component, is particularly instructive. In fact, while the DF of the $\gamma = 1$ density distribution diverges at high (relative) energies in both the one-component and the halo-dominated cases (Fig. 2), the DF of the $\gamma = 0$ model is divergent for high energies in the one-component case, but *finite* in the halo-dominated one (Fig. 3). Moreover, when the $\gamma = 1$ halo concentration increases (i.e., when $\beta = r_0/r_1$ increases), the central value of the DF associated with the $\gamma = 0$ density profile decreases monotonically, and for β greater than the above-mentioned critical value it becomes negative, revealing the model inconsistency. It must be stressed that a similar behavior was found in the numerical investigation of consistency of King (1972) and quasi-isothermal halos added to a de Vaucouleurs (1948) density distribution carried out by CP92. Note also how the decrease of the central value of the DF for increasing halo concentration is reminiscent of that found by C96 for (1, 1) models, even if in that case the transition was found to be more discontinuous: the DF of a $\gamma = 1$ component in (1, 1) models remains divergent at the center for all finite concentrations of the other $\gamma = 1$ component, and becomes exactly zero at the center only when the halo is reduced to a central BH (see Fig. 2 of C96). The qualitative discussion above can be put on more quantitative grounds. In fact, in the halo-dominated case, the central value of the DF of the $\gamma = 0$ component is easily derived for a generic β using the formulae given in § 4.2:

$$\tilde{f}_i^0 = \frac{3\mu}{8\sqrt{2}\pi^3} \begin{cases} -\dfrac{3(64\beta^3 - 240\beta^2 + 280\beta - 105)}{32(1-\beta)^{5/2}\beta^{9/2}} \tan^{-1}\sqrt{\dfrac{1-\beta}{\beta}} - \dfrac{16\beta^3 - 328\beta^2 + 630\beta - 315}{32(1-\beta)^2\beta^4}, & \text{if } 0 < \beta < 1, \\ \dfrac{64}{5}, & \text{if } \beta = 1, \\ -\dfrac{3(64\beta^3 - 240\beta^2 + 280\beta - 105)}{32(\beta-1)^{5/2}\beta^{9/2}} \tanh^{-1}\sqrt{\dfrac{\beta-1}{\beta}} - \dfrac{16\beta^3 - 328\beta^2 + 630\beta - 315}{32(\beta-1)^2\beta^4}, & \text{if } \beta > 1, \end{cases} \tag{36}$$

and

$$\tilde{f}_a^0 = \frac{3\mu}{8\sqrt{2}\pi^3} \begin{cases} \dfrac{3(8\beta^2 - 12\beta + 5)}{32(1-\beta)^{5/2}\beta^{5/2}} \tan^{-1}\sqrt{\dfrac{1-\beta}{\beta}} + \dfrac{(4\beta-3)(2\beta-5)}{32(1-\beta)^2\beta^2}, & \text{if } 0 < \beta < 1, \\ \dfrac{4}{5}, & \text{if } \beta = 1, \\ \dfrac{3(8\beta^2 - 12\beta + 5)}{32(\beta-1)^{5/2}\beta^{5/2}} \tanh^{-1}\sqrt{\dfrac{\beta-1}{\beta}} + \dfrac{(4\beta-3)(2\beta-5)}{32(\beta-1)^2\beta^2}, & \text{if } \beta > 1. \end{cases} \tag{37}$$

The limiting value for β in the isotropic case is obtained by numerically solving the equation $\tilde{f}_i^0 = 0$ for $\beta > 1$. In Figure 4 (where the high-concentration case corresponding to $\beta > 1$ is shown), the decrease of $\tilde{f}_i^0$ when β increases is apparent.

The second important point addressed by using the DFs is the study of the *combined* effect of orbital anisotropy and halo concentration in determining the consistency of the two (1, 0) model components. We cannot expect a simple behavior, because (as should be clear from the previous sections) halo concentration and anisotropy affect the DF in *different* regions of the phase space, i.e., the high-energy regions of the DF are more sensitive to concentration effects, while the OM orbital anisotropy acts mainly at intermediate energies. The simplest way to summarize the results is to express the consistency limitations in terms of the anisotropy radius of each component as a function of β, determining in the parameter space (s_a, β) the critical regions where the models are consistent. This approach is particularly useful because it is independent of the specific form of the density profile of the investigated model; the positivity requirement for each DF of an OM multicomponent system over all the phase space can be expressed in terms of the anisotropy radius as a function of the other model parameters, due to the simple appearance of s_a in equation (20).

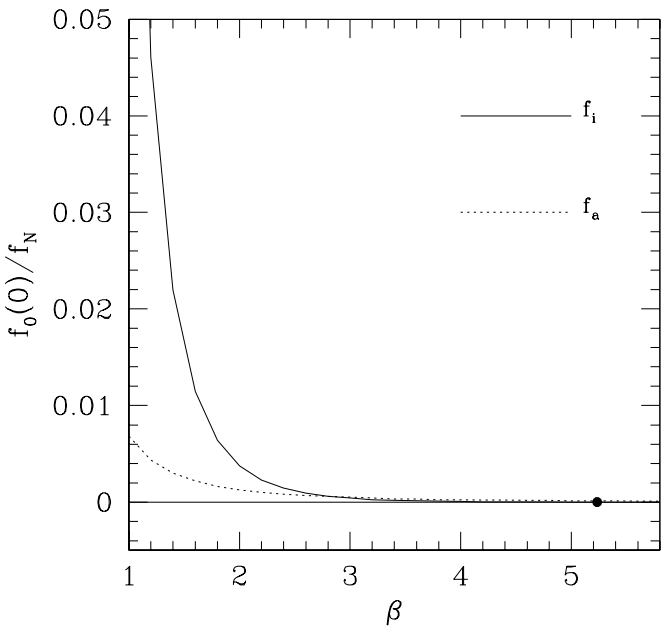

FIG. 4.—Central value of the dimensionless isotropic (*solid line*; eq. [36]) and anisotropic (*dotted line*; eq. [37]) parts of the DF for the halo-dominated $\gamma = 0$ model, as a function of $\beta = r_0/r_1$, for $\beta \geq 1$.

In fact, let A_+ be the set defined by the property that $f_i > 0$ for all $v \in A_+$. Then, from equation (20),

$$s_a \geq s_{ac}^- = \sqrt{\max\left\{0, \sup\left[-\frac{f_a(v)}{f_i(v)}\right]_{v \in A_+}\right\}} \tag{38}$$

is a first condition to be satisfied. Obviously, when $f_i > 0$ over all the phase space (the common situation), A_+ coincides with the total range of variation for v, and equation (38) is also the *only* condition to be checked for the model consistency. In this case equation (38) shows that there is *at most* a lower bound for the anisotropy radius, s_{ac}^-. This is the case, for example, for the $\gamma = 1$ component in (1, 0) and (1, 1) models, or for one-component anisotropic γ models.

When the set A_- (complementary to A_+) is not empty, i.e., when $f_i < 0$ over some region of phase space, a second inequality, derived from equation (20), must necessarily be verified:

$$s_a \leq s_{ac}^+ = \sqrt{\inf\left[\frac{f_a(v)}{|f_i(v)|}\right]_{v \in A_-}} . \tag{39}$$

A general consequence of equations (38) and (39), valid for *all* single- or multicomponent spherically symmetric, radially anisotropic OM models, is that the allowed region for consistency in the anisotropy space is given by $s_{ac}^- < s_a < s_{ac}^+$. Moreover, if $f_a < 0$ for all $v \in A_-$ or $s_{ac}^+ < s_{ac}^-$, then the proposed model is inconsistent.

The quantitative trend of s_{ac}^- for the $\gamma = 1$ density distribution with a dominant $\gamma = 0$ halo is shown in Figure 5*a* (*solid line*); for a given β, all values of s_a higher than the critical curve are acceptable. Note that an increase in the halo concentration (a decreasing β) produces an increase of s_{ac}^-, i.e., a very concentrated halo makes the other component more sensitive to anisotropy effects, a behavior qualitatively anticipated in § 4.1, and already found for (1, 1) models (C96, Fig. 5).

A more complicated (and more interesting) case is presented by the halo-dominated $\gamma = 0$ model. In this case we already know that, due to the halo concentration, even the isotropic case can be inconsistent, i.e., $f_i < 0$. This means that s_{ac}^+ must also be considered. The trend of s_{ac}^- is shown in Figures 5*a* and 5*b* (*dotted line*); as in the previous case, an increase of the minimum anisotropy radius corresponds to an increasing halo concentration (i.e., to an increasing β). As β increases above the critical value $\simeq 5.233$, f_i becomes negative at the center, and the isotropic $\gamma = 0$ component becomes inconsistent; in Figure 5*a* this region is contained in the box at the top–right, which is enlarged in Figure 5*b*. Here the dotted line again shows s_{ac}^-, and the dashed line represents s_{ac}^+; for $5.233 \lesssim \beta \lesssim 6.15$, the inequality $s_{ac}^- < s_{ac}^+$ holds, and according to equations (38) and (39) the region between the two curves corresponds to consistent $\gamma = 0$ components. This is a quite counterintuitive example of the combined effect of an external potential and anisotropy on the consistency of an anisotropic galaxy model, in which an otherwise inconsistent isotropic model is made consistent by orbital anisotropy! Finally, for $\beta \gtrsim 6.15$ no physically acceptable $\gamma = 0$ components are possible, even considering the effect of anisotropy.

A question arises: how well does the asymptotic analysis obtained in the limit of dominant halos compare to the more realistic cases of halos with finite mass? An answer can be obtained by inspection of Figure 5*a*, in which the dashed lines represent the limits on the anisotropy radius obtained when considering a halo ten times as massive as the component investigated. Note that when the halo is *more concentrated* than the considered density component (large β in the case of a

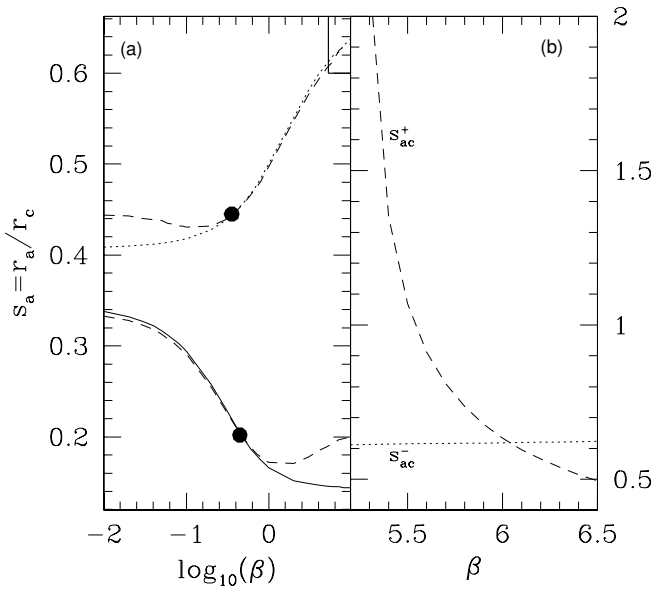

FIG. 5.—Minimum value for the anisotropy radius of both components of (1, 0) models in the case of a dominant halo, as a function of $\beta = r_0/r_1$. The anisotropy radius is normalized to the scale length of the specific component. In (*a*) the solid line shows the $\gamma = 1$ component, and the dotted line the $\gamma = 0$ component. The two dashed lines represent the same quantities when the halo mass is 10 times the mass of the specific component. The filled circles show the critical values of s_a for the one-component models. Panel (*b*) is an enlargement of the small window at the top right of (*a*). The dashed line shows the upper limit on s_a due to the halo concentration effect.

$\gamma = 0$ model [Fig. 5*a*, *dotted line*] and small β for the $\gamma = 1$ model [*solid line*]), the curves corresponding to the asymptotic analysis and the dashed curves are indistinguishable for any practical application. On the other hand, a small departure appears when the halo scale length is substantially larger than that of the considered density component, with the dashed curves approaching the critical value for the anisotropy radius corresponding to the one-component model (Fig. 5*a*, *two filled circles*). This is an obvious behavior, since for any *finite* value of the halo mass, its gravitational effect becomes weaker and weaker for larger and larger halo scale lengths.

6. CONCLUSIONS

In this paper, an extensive analytical investigation of the phase space of two-component spherical galaxy models composed of the sum of a Hernquist density distribution and a $\gamma = 0$ model with different physical scales is carried out. Following the simple Osipkov-Merritt parameterization, a variable amount of orbital anisotropy is allowed in each component. For these models, other important properties useful in applications—the velocity dispersion components and the various energy terms entering the scalar virial theorem—can be expressed analytically, and are given in Appendix C. The main results can be summarized as follows:

1. The necessary and sufficient conditions that the model parameters must satisfy in order to correspond to a (1, 0) system for which the two physically distinct components have a positive DF are analytically derived using the method introduced in CP92. Some conditions are obtained for the wider class of two-component (γ_1, γ_2) models [of which the (1, 0) models are a special case]. In particular, it is shown that the DF of the γ_1 component in isotropic (γ_1, γ_2) models is nowhere negative, independent of the mass and concentration of the γ_2 component, whenever $1 \leq \gamma_1 < 3$ and $0 \leq \gamma_2 \leq \gamma_1$. As a special application of this result, it follows that a BH of any mass can be consistently added at the center of any isotropic member of the γ family of models when $1 \leq \gamma < 3$. Two important consequences follow. The first is that the consistency of isotropic (1, 1) [or (1, BH)] models proved in C96 using an "ad hoc" technique is not exceptional, but a common property of a large class of two-component γ models: for example, isotropic two-component Jaffe ($\gamma = 2$) or Jaffe + BH models can also be safely assembled. The second is that in two-component isotropic models, the component with the steeper central density distribution is usually the most robust against inconsistency.

2. It is shown that an analytic estimate of a minimum value of s_a for one-component γ models with a massive (dominant) BH at their center can be explicitly found. As expected, this minimum value decreases for increasing γ.

3. It is shown that the analytic expression for the DF of (1, 0) models with general OM anisotropy can be found in terms of elliptic functions. The special cases in which each one of the two density components are embedded in a dominant halo are also discussed; under this assumption, the DFs can be expressed using just elementary functions, allowing a detailed analytical investigation.

4. The region of the parameter space in which (1, 0) models are consistent is explored using the derived DFs; it is shown that, unlike the $\gamma = 1$ component, the $\gamma = 0$ component becomes inconsistent when the halo is sufficiently concentrated, even in the isotropic case. This is an explicit example (albeit not so extreme) of the result found by CP92 that numerically proved

the impossibility of adding a King or a quasi-isothermal halo to a de Vaucouleurs galaxy. In such models, the (isotropic) de Vaucouleurs galaxy was found instead to be consistent over all the parameter space.

5. Finally, the combined effect of halo concentration and orbital anisotropy is investigated. The trend of the minimum value for the anisotropy radius as a function of the halo concentration is qualitatively similar in both components, and similar to that found for (1, 1) models in C96: a more diffuse halo allows a larger amount of anisotropy. A qualitatively new behavior is found and explained by investigating the DF of the $\gamma = 0$ component in the halo-dominated case for high halo concentrations. It is analytically shown that there exists a small region in the parameter space where a sufficient amount of *anisotropy* can compensate for the inconsistency produced by the halo concentration on the structurally analogous but isotropic case.

As a final remark, it may be useful to point out some general trends that emerge when comparing different one- and two-component models with OM anisotropy, such as those investigated numerically in CP92 and CL97 and analytically in C96 and in this paper. The first common trend is that OM anisotropy produces a negative DF outside the galaxy center, while the halo concentration affects mainly the DF at high (relative) energies. The second is that the possibility of sustaining a strong degree of anisotropy is weakened by the presence of a very concentrated halo. The third is that in two-component models, in cases of very different density profiles in the central regions, the component with the flatter density is the most "delicate" and can easily be found to be inconsistent; particular attention should be paid in constructing such models.

I would like to thank Giuseppe Bertin, Laura Greggio, and Silvia Pellegrini for helpful comments and discussions. The referee, Stephen Levine, is especially thanked for his comments that greatly improved the paper. This work has been partially supported by contracts ASI-95-RS-152, ASI-ARS-96-70, and MURST-Cofin98.

APPENDIX A

CONSISTENCY REQUIREMENTS

A1. THE NC AND WSC FOR ONE-COMPONENT γ MODELS

The NC (eq. [4]) for the anisotropic (one-component) γ models imposes a limitation on the anisotropy radius:

$$s_a^2 \geq \frac{s^2(2-\gamma-2s)}{\gamma+4s}, \qquad 0 \leq s \leq \infty . \tag{A1}$$

This inequality is true for s_a^2 larger than or equal to the maximum of the function on the right-hand side of equation (A1). For $2 \leq \gamma$, the right-hand side is strictly negative, and so all values of s_a satisfy the NC. When $0 \leq \gamma < 2$, the maximum is reached at

$$s_M(\gamma) = \frac{4-5\gamma+\sqrt{(4-\gamma)(4+7\gamma)}}{16}, \tag{A2}$$

which after substitution in equation (A1) gives equation (13).

The WSC (eq. [6]) applied to the anisotropic one-component γ models gives the following inequality:

$$s_a^2 \geq \frac{s^3(3-\gamma-s)}{6s^2+2(1+\gamma)s+\gamma}, \qquad 0 \leq s \leq \infty . \tag{A3}$$

After differentiation, one is left with the discussion of a cubic equation. Its discriminant is negative for $0 \leq \gamma < (\sqrt{73}-5)/8$ and positive for $(\sqrt{73}-5)/8 < \gamma < 3$. In the first case, two of the three real solutions are negative, and the maximum of the right-hand side of equation (A3) is reached at

$$s_M(\gamma) = \frac{1-\gamma}{3} + \frac{2\sqrt{4-\gamma}}{3} \cos\left[\frac{1}{3}\tan^{-1}\frac{\sqrt{(15-4\gamma)(3-\gamma)(3-5\gamma-4\gamma^2)}}{11+11\gamma-4\gamma^2}\right]. \tag{A4}$$

In the second case, discarding the two complex conjugates roots, and defining

$$s_0 = (4-\gamma)[11+11\gamma-4\gamma^2+\sqrt{(15-4\gamma)(3-\gamma)(4\gamma^2+5\gamma-3)}], \tag{A5}$$

the maximum is reached at

$$s_M(\gamma) = \frac{s_0^{1/3}}{6} + \frac{1-\gamma}{3} + \frac{2(4-\gamma)}{3s_0^{1/3}}. \tag{A6}$$

Finally, when $\gamma = (\sqrt{73} - 5)/8 \simeq 0.443$, $s_M = (\sqrt{73} + 3)/8 \simeq 1.443$.

A2. THE SSC FOR THE $\gamma = 0$ AND $\gamma = 1$ MODELS

The SSC (eq. [5]) applied to the anisotropic one-component $\gamma = 0$ model gives the following inequality:

$$s_a^2 \geq \frac{3s^2(1 + 2s - s^2)}{14s^2 + 10s + 2}, \qquad 0 \leq s \leq \infty . \tag{A7}$$

The maximum of the right-hand side of equation (A7) can be obtained explicitly by solving a fourth-degree equation. The numerical value of the only physically acceptable solution is

$$s_M(0) \simeq 1.3149 , \tag{A8}$$

which after back-substitution in equation (A7) gives equation (15).

The SSC applied to the anisotropic one-component $\gamma = 1$ model gives the following inequality:

$$s_a^2 \geq \frac{3s^3(3 - 2s)}{28s^2 + 17s + 4}, \qquad 0 \leq s \leq \infty . \tag{A9}$$

After differentiation, discarding the two complex conjugate roots of the resulting cubic equation, and defining

$$s_0 = 681939 + 84\sqrt{35887965} , \tag{A10}$$

the maximum of the right-hand side of equation (A9) is reached at

$$s_M(1) = \frac{s_0^{1/3}}{168} - \frac{3}{56} + \frac{1987}{56 s_0^{1/3}} \simeq 0.9116 , \tag{A11}$$

which after back substitution in equation (A9) gives equation (16).

A3. THE WSC FOR ISOTROPIC (γ_1, γ_2) MODELS

With the aid of the WSC, the positivity of the DF for the γ_1 density distribution of the globally isotropic two-component (γ_1, γ_2) models, where $1 \leq \gamma_1 < 3$ and $0 \leq \gamma_2 \leq \gamma_1$, is here discussed. Having computed the derivatives prescribed by equation (6), we must investigate the positivity of a rational expression whose denominator is strictly positive for all (γ_1, γ_2) and for all (s, β); the numerator factorizes in a strictly positive function and in a transcendental expression. Defining $\gamma_1 = 1 + \epsilon_1$ (with $0 \leq \epsilon_1 < 2$) and $\gamma_2 = \gamma_1 - \epsilon_2$ (with $0 \leq \epsilon_2 \leq \gamma_1$), the transcendental factor reads

$$2(s + \beta)^4(1 + 1/s)^{\gamma_1}[6s^2 + 2(1 + \gamma_1)s + \gamma_1] + \mu(s + 1)^3(1 + \beta/s)^{\gamma_2} F(s, \beta, \gamma_1, \gamma_2) , \tag{A12}$$

where the first addend is strictly positive, and

$$F(s, \beta, \gamma_1, \gamma_2) = 12s^3 + 4[(5 - \epsilon_1 + \epsilon_2)\beta + 2\epsilon_1]s^2 + [(10 + 5\epsilon_1 - \epsilon_1^2 + 5\epsilon_2 + \epsilon_1\epsilon_2)\beta + \epsilon_1\gamma_1]s + \beta\gamma_1(2 + \epsilon_2) . \tag{A13}$$

In the range of values for ϵ_1 and ϵ_2, the positivity of F is easily proved for all $(s, \beta) \geq 0$, and so equation (6) is verified for all (μ, β).

The application of the WSC to the globally isotropic $\gamma = 0$ component of a (1, 0) model is simple, leading to the discussion of

$$\mu \geq \frac{-(3s + 5 - 2\beta)(s + \beta)^3}{(3s + \beta)(s + 1)^3}, \qquad 0 \leq s \leq \infty . \tag{A14}$$

First, note that for $\beta < 5/2$ the previous inequality is satisfied for all $\mu \geq 0$. When $\beta \geq 5/2$, the maximum of the right-hand side of equation (A14) over the interval $0 \leq s \leq \infty$ is reached at $s = 0$, and so the condition given in equation (17) is derived.

A4. THE WSC FOR ANISOTROPIC (γ, BH) MODELS

In this case we assume in equation (6) $M_T = M_{\rm BH}$, and from the previous discussion we restrict it to γ models with $1 \leq \gamma < 3$. After the computation of the derivatives, we must investigate the inequality

$$s_a^2 \geq \frac{s^2[(3 - \gamma)(\gamma - 2) + 4(3 - \gamma)s - 2s^2]}{12s^2 + 8(\gamma - 1)s + \gamma(\gamma - 1)}, \qquad 0 \leq s \leq \infty . \tag{A15}$$

After differentiation, one is left with the discussion of a quartic equation, and it can be shown that there exists only one maximum, located at $s_M = s_M(\gamma) \geq 0$. The explicit expression for $s_M(\gamma)$ is not very useful and so is not reported here. In any

case, of interest are the explicit values of $s_M(\gamma)$ for $\gamma = (1,2,3)$. After easy computations, one finds

$$s_M(1) = 2\,, \qquad s_M(2) = \frac{(54 + 6\sqrt{33})^{1/3}}{6} + \frac{2}{(54 + 6\sqrt{33})^{1/3}} \simeq 1.191\,, \qquad s_M(3) = 0\,, \tag{A16}$$

which after substitution in equation (18) give the values reported in Table 1.

APPENDIX B

THE DF OF (1, 0) MODELS

Here the main steps required for the determination of the DF of each component of (1, 0) models are briefly described. Changing the integration variable from the total potential to the radius, and after normalization to the physical scales of the $\gamma = 1$ component, equation (2) becomes

$$f(Q) = \frac{f_N}{\sqrt{8}\pi^2}\left(\frac{d\tilde{Q}}{dv}\right)^{-1}\frac{d\tilde{F}(v)}{dv}\,, \tag{B1}$$

where the relation between v and $\tilde{Q}$ is given by equation (19), and

$$\tilde{F}(v) = -\int_v^\infty \frac{d\tilde{\varrho}}{ds}\frac{ds}{\sqrt{\tilde{\Psi}_T(v) - \tilde{\Psi}_T(s)}}\,. \tag{B2}$$

Note that a negative sign appears in front of the integral above; this is due to the monotonic decrease of the relative potential with radius. From equations (11) and (12),

$$\frac{1}{\sqrt{\tilde{\Psi}_T(v) - \tilde{\Psi}_T(s)}} = \sqrt{\frac{1+s}{s-v}}\,\frac{\sqrt{2(1+v)}(\beta+v)(\beta+s)}{\sqrt{As^2 + Bs + C}}\,, \tag{B3}$$

where A, B, and C are constants depending on (μ, β, v). Finally, observing that for each component $d\tilde{\varrho}/ds$ is a rational function of s, with the standard change of the integration variable $(1+s)/(s-v) = t^2$ it follows that the integral in equation (B2) can be expressed in terms of elliptic integrals.

B1. THE DF OF THE ONE-COMPONENT $\gamma = 1$ MODEL AS A FUNCTION OF v

In this case, in equation (B1)

$$\tilde{Q} = \frac{1}{1+v}\,; \qquad \left(\frac{d\tilde{Q}}{dv}\right)^{-1} = -(1+v)^2\,. \tag{B4}$$

After differentiation under the integral in equation (B2), with $\tilde{\varrho}$ given by equations (3) and (7) and $\tilde{\Psi}_T = \tilde{\Psi}_1$, and after a partial fraction decomposition of the rational part of the integrand, one obtains

$$\tilde{F}_i(v) = -\frac{\sqrt{1+v}}{2\pi}\left[\frac{2}{15}\frac{15v^2 + 50v + 59}{(1+v)^3} - \frac{1}{v} - \frac{1+v}{v^{3/2}}\tan^{-1}\frac{1}{\sqrt{v}}\right] \tag{B5}$$

and

$$\tilde{F}_a(v) = -\frac{\sqrt{1+v}}{2\pi}\frac{8}{15}\frac{1-5v}{(1+v)^3}\,. \tag{B6}$$

A check of the derived formulae is obtained by substitution of $v = v(\tilde{Q})$ as given by inverting the first of equations (B4) and comparing the result with the DF given in H90.

B2. THE DF FOR THE ONE-COMPONENT $\gamma = 0$ MODEL AS A FUNCTION OF v

In this case, the scale length r_0 of the $\gamma = 0$ component and its mass M_0 are assumed as physical scales, and so $f_N = (M_0/r_0^3)(GM_0/r_0)^{-3/2}$. This is formally equivalent to assuming $\beta = 1$ and $\mu = 1$ in equations (10) and (12), and so in equation (B1),

$$\tilde{Q} = \frac{1+2v}{2(1+v)^2}\,; \qquad \left(\frac{d\tilde{Q}}{dv}\right)^{-1} = -\frac{(1+v)^3}{v}\,. \tag{B7}$$

After differentiation under the integral in equation (B2) with $\tilde{\varrho}$ given by equations (3) and (9) and $\tilde{\Psi}_T = \tilde{\Psi}_0$, and after a partial fraction decomposition of the rational part of the integrand, one obtains

$$\tilde{F}_i(v) = -\frac{3\sqrt{2}}{4\pi}\left[\frac{2\sqrt{1+2v}(15v^2+22v+11)}{3(1+v)^3} - \frac{4(5v^2+4v+2)}{(1+v)^2}\tanh^{-1}\frac{1}{\sqrt{1+2v}}\right] \tag{B8}$$

and

$$\tilde{F}_a(v) = -\frac{3\sqrt{2}}{4\pi}\left[\frac{\sqrt{1+2v}(9v^2+2v+1)}{3(1+v)^3} - \frac{6v^2}{(1+v)^2}\tanh^{-1}\frac{1}{\sqrt{1+2v}}\right]. \tag{B9}$$

A check of the derived formulae is obtained by substitution of $v = v(\tilde{Q})$, as given by inverting the first of equations (B7), and comparing the result with the DF given in D93.[5]

APPENDIX C

THE VELOCITY DISPERSIONS AND VIRIAL QUANTITIES

Here I present the main dynamical quantities of the model discussed in this paper. The radial component σ_r^2 of the velocity dispersion $\sigma^2 = \sigma_r^2 + \sigma_t^2$ in the OM parameterization can be written for each component as

$$\rho(r)\sigma_r^2(r) = \frac{A(r) + r_a^2 I(r)}{r^2 + r_a^2}, \tag{C1}$$

where

$$A(r) = G\int_r^\infty \rho(r)M_T(r)\,dr, \qquad I(r) = G\int_r^\infty \frac{\rho(r)M_T(r)}{r^2}dr, \tag{C2}$$

(Binney & Mamon 1982); once σ_r^2 is obtained, the tangential velocity dispersion is given by

$$\sigma_t^2(r) = \frac{2r_a^2}{r^2 + r_a^2}\,\sigma_r^2(r). \tag{C3}$$

Other quantities of interest in applications, such as the global energies entering the scalar virial theorem, are derived in the following sections.

C1. THE $\gamma = 1$ COMPONENT

Because of the presence of the $\gamma = 0$ component, $\tilde{I}_1 = \tilde{I}_{11} + \mu\tilde{I}_{10}$ and $\tilde{A}_1 = \tilde{A}_{11} + \mu\tilde{A}_{10}$, where the dimensional coefficients of the velocity dispersions and energies are Ψ_N and $U_N = M_1\,\Psi_N$, respectively. After normalization and integration, one finds

$$\tilde{I}_{11} = \frac{1}{2\pi}\ln\left(\frac{1+s}{s}\right) - \frac{12s^3+42s^2+52s+25}{24\pi(1+s)^4}, \qquad \tilde{A}_{11} = \frac{1+4s}{24\pi(1+s)^4}. \tag{C4}$$

The interaction with the $\gamma = 0$ halo is described by the two contributions

$$\tilde{I}_{10} = \frac{3}{\pi(\beta-1)^5}\ln\left(\frac{\beta+s}{1+s}\right) - \frac{(2s+\beta+1)[6s^2+6s(\beta+1)-\beta^2+8\beta-1]}{4\pi(\beta-1)^4(1+s)^2(\beta+s)^2} \tag{C5}$$

and

$$\tilde{A}_{10} = \frac{(\beta^2+4\beta+1)}{2\pi(\beta-1)^5}\ln\left(\frac{\beta+s}{1+s}\right) - \frac{2(\beta^2+4\beta+1)s^3+3(\beta+1)(\beta^2+4\beta+1)s^2+2\beta(5\beta^2+8\beta+5)s+6\beta^2(\beta+1)}{4\pi(\beta-1)^4(\beta+s)^2(1+s)^2}. \tag{C6}$$

When $\beta = 1$,

$$\tilde{I}_{10} = \frac{1}{10\pi(1+s)^5}, \qquad \tilde{A}_{10} = \frac{10s^2+5s+1}{60\pi(1+s)^5}. \tag{C7}$$

[5] The anisotropic part of the DF given in D93 should be multiplied by 2.

The gravitational energy of the $\gamma = 1$ component is given by $\tilde{U}_1 = \tilde{U}_{11} + \mu\tilde{U}_{10}$, where $U_{11} = -2\pi \int \rho_1 \Psi_1 r^2 dr$ is the contribution due to self-interaction, and $U_{10} = -4\pi \int \rho_1 \Psi_0 r^2 dr$ is due to the $\gamma = 0$ halo potential. After normalization,

$$\tilde{U}_{11} = -\frac{1}{6}, \qquad \tilde{U}_{10} = -\frac{\beta^2 - 5\beta - 2}{2(\beta - 1)^3} - \frac{3\beta \ln \beta}{(\beta - 1)^4}, \tag{C8}$$

with $\tilde{U}_{10} = -\frac{1}{4}$ for $\beta = 1$. As is well known, the scalar virial theorem for a multicomponent system reads $\tilde{K}_1 = (|\tilde{U}_{11}| + \mu|\tilde{W}_{10}|)/2$, where the interaction energy is $W_{10} = 4\pi \int r^3 \rho_1 (d\Psi_0/dr) dr$, and after normalization

$$\tilde{W}_{10} = -\frac{\beta^2 + 10\beta + 1}{(\beta - 1)^4} + \frac{6\beta(\beta + 1)\ln \beta}{(\beta - 1)^5}, \tag{C9}$$

with $\tilde{W}_{10} = -1/10$ for $\beta = 1$.

C2. THE $\gamma = 0$ COMPONENT

In this section the normalization constants are the physical scales of the $\gamma = 0$ component, i.e., $s = r/r_0$, $\mu = M_1/M_0$, and $\beta = r_1/r_0$. Consistently with this choice, $\Psi_N = GM_0/r_0$, $U_N = M_0 \Psi_N$, $\tilde{I}_0 = \tilde{I}_{00} + \mu\tilde{I}_{01}$, and $\tilde{A}_0 = \tilde{A}_{00} + \mu\tilde{A}_{01}$. After normalization and integration, one finds

$$\tilde{I}_{00} = \frac{1 + 6s}{40\pi(1 + s)^6}, \qquad \tilde{A}_{00} = \frac{20s^3 + 15s^2 + 6s + 1}{80\pi(1 + s)^6}. \tag{C10}$$

The interaction with the $\gamma = 1$ halo is described by the two contributions

$$\tilde{I}_{01} = \frac{3}{\pi(\beta - 1)^5} \ln\left(\frac{1 + s}{\beta + s}\right) + \frac{12s^3 + 6(\beta + 5)s^2 - 2(\beta^2 - 8\beta - 11)s + \beta^3 - 5\beta^2 + 13\beta + 3}{4\pi(\beta - 1)^4(1 + s)^3(\beta + s)}, \tag{C11}$$

and

$$\tilde{A}_{01} = \frac{3\beta(\beta + 1)}{2\pi(\beta - 1)^5} \ln\left(\frac{1 + s}{\beta + s}\right) + \frac{6\beta(\beta + 1)s^3 + 3\beta(\beta + 5)(\beta + 1)s^2 + (3\beta^3 + 25\beta^2 + 7\beta + 1)s + \beta(\beta^2 + 10\beta + 1)}{4\pi(\beta - 1)^4(1 + s)^3(\beta + s)}. \tag{C12}$$

When $\beta = 1$,

$$\tilde{I}_{01} = \frac{3}{20\pi(1 + s)^5}, \qquad \tilde{A}_{01} = \frac{10s^2 + 5s + 1}{40\pi(1 + s)^5}. \tag{C13}$$

The gravitational energy of the $\gamma = 0$ component is given by $\tilde{U}_0 = \tilde{U}_{00} + \mu\tilde{U}_{01}$, where $U_{00} = -2\pi \int \rho_0 \Psi_0 r^2 dr$ is the contribution due to self-interaction, and $U_{01} = -4\pi \int \rho_0 \Psi_1 r^2 dr$ is due to the $\gamma = 1$ halo potential. After normalization,

$$\tilde{U}_{00} = -\frac{1}{10}, \qquad \tilde{U}_{01} = -\frac{2\beta^2 + 5\beta - 1}{2(\beta - 1)^3} + \frac{3\beta^2 \ln \beta}{(\beta - 1)^4}, \tag{C14}$$

with $\tilde{U}_{01} = -\frac{1}{4}$ for $\beta = 1$, obviously equal to $\tilde{U}_{10}$. In this case the interaction energy is $W_{01} = 4\pi \int r^3 \rho_0 (d\Psi_1/dr) dr$, and the virial theorem is $\tilde{K}_0 = (|\tilde{U}_{00}| + \mu|\tilde{W}_{01}|)/2$; after normalization one obtains

$$\tilde{W}_{01} = \frac{17\beta^2 + 8\beta - 1}{2(\beta - 1)^4} - \frac{3\beta^2(\beta + 3)\ln \beta}{(\beta - 1)^5}. \tag{C15}$$

For $\beta = 1$, $\tilde{W}_{01} = -3/20$.

REFERENCES

Bertin, G., Saglia, R. P., & Stiavelli, M. 1992, ApJ, 384, 423
Bertin, G., & Stiavelli, M. 1984, A&A, 137, 26
Bertin, G., et al. 1994, A&A, 292, 381
Binney, J. 1981, MNRAS, 196, 455
Binney, J., & Mamon, G. 1982, MNRAS, 200, 361
Binney, J., & Tremaine, S. 1987, Galactic Dynamics (Princeton: Princeton Univ. Press) (BT87)
Buote, D. A., & Canizares, R. C. 1997, ApJ, 474, 650
Byun, Y. I., Grillmair, C., Faber, S. M., Ajhar, E. A., Dressler, A., Kormendy, J., Lauer, T. R., Richstone, D. O., & Tremaine, S. D. 1996, AJ, 111, 1889
Carollo, C. M. 1993, Ph.D. thesis, Ludwig-Maximilians Univ. (Munich)
Carollo, C. M., de Zeeuw, P. T., & van der Marel, R. P. 1995a, MNRAS, 276, 1131
Carollo, C. M., de Zeeuw, P. T., van der Marel, R. P., Danziger, I. J., & Qian, E. E. 1995b, ApJ, 441, L25
Carollo, C. M., & Stiavelli, M. 1998, AJ, 115, 2306
Ciotti, L. 1996, ApJ, 471, 68 (C96)
Ciotti, L., & Lanzoni, B. 1997, A&A, 321, 724 (CL97)
Ciotti, L., & Pellegrini, S. 1992, MNRAS, 255, 561 (CP92)
de Vaucouleurs, G. 1948, Ann. d'Astrophys., 11, 247
de Zeeuw, P. T. 1996, Proc. 36th Herstmonceux Conf., Gravitational Dynamics, ed. O. Lahav, E. Terlevich, & R. Terlevich (Cambridge: Cambridge Univ. Press), 1
Dehnen, W. 1993, MNRAS, 265, 250 (D93)
Dubinski, J., & Carlberg, R. G. 1991, ApJ, 378, 496
Eddington, A. S. 1916, MNRAS, 76, 572
Evans, N. 1993, MNRAS, 260, 191

Ferrarese, L., van den Bosch, F. C., Ford, H. C., Jaffe, W., & O'Connell, R. W. 1994, AJ, 108, 1598
Gerhard, O., Jeske, G., Saglia, R. P., & Bender, R. 1998, MNRAS, 295, 197
Harms, R. J., et al. 1994, ApJ, 435, L35
Hernquist, L. 1990, ApJ, 536, 359 (H90)
Hiotelis, N. 1994, A&A, 291, 725
Jaffe, W. 1983, MNRAS, 202, 995
Jaffe, W., Ford, H. C., O'Connell, R. W., van den Bosch, F. C., & Ferrarese, L. 1994, AJ, 108, 1567
King, I. 1972, ApJ, 174, L123
Kormendy, J., et al. 1995, in IAU Symp. 171, New Light on Galaxy Evolution, ed. R. Bender & R. L. Davies (Dordrecht: Kluwer), 105
Lauer, T. R., et al. 1995, AJ, 110, 2622
Loewenstein, M., & White, R. E., III. 1999, preprint (astro-ph/9901242)
Merritt, D. 1985a, AJ, 90, 1027
Merritt, D. 1985b, MNRAS, 214, 25P
Møller, P., Stiavelli, M., & Zeilinger, W. W. 1995, MNRAS, 276, 979
Navarro, J. F., Frenk, C. S., & White, S. D. M. 1997, ApJ, 490, 493
Osipkov, L. P. 1979, Pis'ma Astron. Zh., 5, 77
Pellegrini, S., & Ciotti, L. 1998, A&A, 333, 433
Richstone, D. O. 1998, in IAU Symp. 184, The Central Region of the Galaxy and Galaxies, ed. Y. Sofue, in press
Tremaine, S. D., Richstone, D. O., Byun, Y. I., Dressler, A., Faber, S. M., Grillmair, C., Kormendy, J., & Lauer, T. R. 1994, AJ, 107, 634
van der Marel, R. P., de Zeeuw, P. T., & Rix, H.-W. 1997a, ApJ, 488, 119
van der Marel, R. P., de Zeeuw, P. T., Rix, H.-W., & Quinlan, G. D. 1997b, Nature, 385, 610
White, S. D. M. 1996, Proc. 36th Herstmonceux Conf., Gravitational Dynamics, ed. O. Lahav, E. Terlevich, & R. Terlevich (Cambridge: Cambridge Univ. Press), 121